JOURNAL OF GEOPHYSICAL RESEARCH, VOL. 95, NO. B5, PAGES 6779–6786, MAY 10, 1990

AD-A228 685

Obtaining Earth Surface and Spatial Deflections of the Vertical From Free-Air Gravity Anomaly and Elevation Data Without Density Assumptions

DAVID M. GLEASON

Geophysics Laboratory, Hanscom Air Force Base, Bedford, Massachusetts

Moritz (1980) presents a density-free scheme allowing for the analytical or regular continuation of a given set of free-air gravity anomalies, referenced to the ground, to any desired level surface if a corresponding set of elevations (e.g., above mean sea level) is available. An efficient spectral implementation of this scheme is discussed by Sideris (1987). A subsequent spectral execution of the planar Vening-Meinez equation on the continued anomalies yields deflections of the vertical on the chosen level surface. The deflections are brought back to the Earth's surface via a spectrally implemented Taylor series. Deflections at a constant altitude above the level surface are obtained through a routine spectral execution of the planar upward continuation integral. Two sites, having diverse topographies, were surveyed for 1 arc min by 1 arc min mean free-air anomaly and elevation values and for smaller sets of astronomically determined deflections to serve as control or "truth" values. In a topographically tranquil but gravimetrically turbulent Oklahoma site the overall RMS of the differences between true and predicted deflections was 0.3 arc secs and in a rugged New Mexico site it was 0.6 arc sec. Accurate first derivative terms (in both continuation steps) require a 1 arc min data set as interpolation-free as possible. A 1 arc min data grid is shown to be insufficient for meaningful computations of the higher order series terms. Potential pitfalls of the two-dimensional fast Fourier transform pair are discussed with an emphasis on unwanted circular convolution effects which, if unaccounted for, can increase the error in individual predicted deflections by as much as 100%.

1. INTRODUCTORY THEORETICAL DISCUSSION

Runge's theorem [cf. *Moritz*, 1980] states one can always find a harmonic function T^*, arbitrarily close to the Earth's external (and harmonic) disturbing potential T, that can be analytically or regularly continued (be it upward or downward) from the Earth's actual surface to any desired level surface. Therefore a converging Taylor series links the observed Δg_P free-air gravity anomaly, referenced to the ground and given by

$$g_{\text{observed at } P} - \gamma_{\text{at the telluroidal point } R}$$

to the anomaly $\Delta g'_{P'}$, referenced to the chosen level surface (see Figure 1 for subscript referrals). *Heiskanen and Moritz* [1967] define the telluroid as a near-ground surface whose normal potential at R is equal to the actual potential at the corresponding ground point P (the points P and R reside on the same ellipsoidal normal) and show how to compute the normal gravity γ_R.

Under such a regular continuation of T, the level surface $\Delta g'$ set reflects the Earth's exterior gravity field. Inserting the $\Delta g'$ set into Stokes' formula yields a potential T' which is harmonic above the chosen level surface (thus unrelated to the Earth's nonharmonic interior field) and which agrees with the actual T on and above the Earth's surface. Therefore any masses existing outside the chosen surface are, in effect, shifted to its interior without changing T on and above the ground. This regular "continuation" of T (and thus Δg) is, at least theoretically, preferable to traditional Bouguer and isostatic "reductions" because the former can be accomplished without any assumptions regarding the densities

of such masses and without approximating the vertical gradient of actual gravity by its normal counterpart $\partial \gamma / \partial z \cong -0.3086$ mGal/m. As shown later in this section, the vertical gradient of anomalous gravity is actually solved for in the continuation process.

The Taylor series of interest is given by

$$\Delta g_P = \Delta g_{P'} + z_P \frac{\partial \Delta g_{P'}}{\partial z} + \frac{1}{2!} z_P^2 \frac{\partial^2 \Delta g_{P'}}{\partial z^2}$$
$$+ \frac{1}{3!} z_P^3 \frac{\partial^3 \Delta g_{P'}}{\partial z^3} + \cdots \quad (1)$$

where

$$z_P = h_P - h' \quad (2)$$

with the heights h_P and h' shown in Figure 1.

An inversion of equation (1) is desired, i.e., a solution for $\Delta g'$ in terms of the observed Δg. Armed with a set of $\Delta g'$ on the level surface approximated by an infinitely extended plane, one can compute the height anomaly ζ, the deflection of the vertical component along the meridian, ξ, and along the prime vertical, η, at any point P' located on the level surface via the planar versions of the Bruns and Vening-Meinez equations [cf. *Bomford*, 1971]

$$\zeta(x_{P'}, y_{P'})$$
$$= \frac{1}{2\pi\gamma} \int_{-\infty}^{\infty} \int_{-\infty}^{\infty} \frac{\Delta g'(x, y)}{[(x_{P'} - x)^2 + (y_{P'} - y)^2]^{1/2}} \, dx \, dy \quad (3)$$

and

This paper is not subject to U.S. copyright. Published in 1990 by the American Geophysical Union.
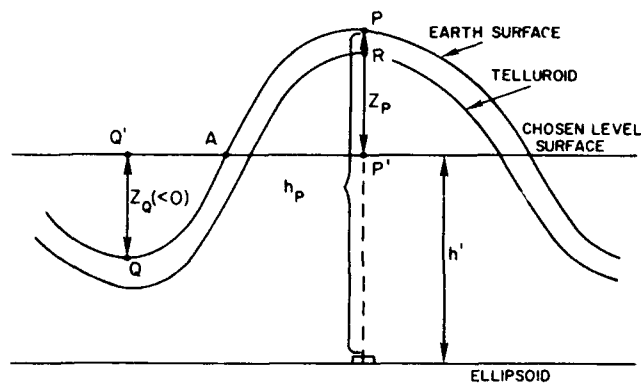
Paper number 89JB03782.

Fig. 1. The applicable surfaces.

$$\begin{Bmatrix} \xi(x_{P'}, y_{P'}) \\ \eta(x_{P}, y_{P'}) \end{Bmatrix} = \frac{1}{2\pi\gamma} \int_{-\infty}^{\infty} \int_{-\infty}^{\infty} \begin{Bmatrix} y_{P'} - y \\ x_{P'} - x \end{Bmatrix}$$

$$\cdot \frac{\Delta g'(x, y)}{[(x_{p'} - x)^2 + (y_{P'} - y)^2]^{3/2}} \, dx \, dy \qquad (4)$$

where γ is some mean value of normal gravity (say, 979,800 mGal). Just as (1) returns one to Δg_P from $\Delta g'_{P'}$, use of similar Taylor series allows one to obtain ζ_P, ξ_P and η_P from $\zeta_{P'}$, $\xi_{P'}$, and $\eta_{P'}$.

Moritz [1980] shows that for any point Q' on the level surface

$$\Delta g'_{Q'} = \sum_{n=0}^{\infty} g^n_{Q'} \qquad (5)$$

where the $g^n_{Q'}$ (superscript combinations involving n or k do not denote exponentiation while those involving r only do) are computed recursively via

$$g^n_{Q'} = -\sum_{r=1}^{n} z^r_{Q'} L_r(g^{n-r}_{Q'}) \qquad (6)$$

where the L_r values are also obtained recursively via

$$L_r(g^k_{Q'}) = \frac{1}{r} L_1[L_{r-1}(g^k_{Q'})] \qquad (7)$$

for any arbitrary k and the function L_1 is defined below by equation (9). The starting values needed to implement (6) and (7) are given by

$$g^0_{Q'} = \Delta g_Q \qquad (8)$$

and

$$L_1[g^0(x_{Q'}, y_{Q'})]$$

$$= \frac{1}{2\pi} \int_{-\infty}^{\infty} \int_{-\infty}^{\infty} \frac{g^0(x, y) - g^0(x_{Q'}, y_{Q'})}{[(x_{Q'} - x)^2 + (y_{Q'} - y)^2]^{3/2}} \, dx \, dy \qquad (9)$$

Notice that (9) is the planar version of the well-known integral expression for the anomalous radial (vertical) gradient $\partial\Delta g/\partial r$ (or $\partial\Delta g/\partial z$) wherein Δg is assumed to be a harmonic function in space. Under the planar approximation

where $\Delta g = -\partial T/\partial z$, such an assumption is appropriate [see *Moritz*, 1980, p. 176]. The geometric kernel of (9), $1/$(distance)^3, dictates $\partial\Delta g/\partial z$ to be a high-frequency/short-wavelength phenomena. *Schwartz* [1984], assuming a widely used model spectrum, shows that over 60% of the value of $\partial\Delta g/\partial z$ is determined by the behavior of the gravity field in the immediate 3 arc min area surrounding the computation point. Thus the g^0 or Δg data in this immediate area must be highly reliable to accurately compute $\partial\Delta g/\partial z$.

Now equations (3) and (4) can be written as

$$\zeta(x_{P'}, y_{P'})$$

$$= \frac{1}{2\pi\gamma} \sum_{n=0}^{\infty} \int_{-\infty}^{\infty} \int_{-\infty}^{\infty} \frac{g^n(x, y)}{[(x_{P'} - x)^2 + (y_{P'} - y)^2]^{1/2}} \, dx \, dy$$

$$(10)$$

and

$$\begin{Bmatrix} \xi(x_{P'}, y_{P'}) \\ \eta(x_{P'}, y_{P'}) \end{Bmatrix} = \frac{1}{2\pi\gamma} \sum_{n=0}^{\infty} \int_{-\infty}^{\infty} \int_{-\infty}^{\infty} \begin{Bmatrix} y_{P'} - y \\ x_{P'} - x \end{Bmatrix}$$

$$\cdot \frac{g^n(x, y)}{[(x_{P'} - x)^2 + (y_{P'} - y)^2]^{3/2}} \, dx \, dy \qquad (11)$$

Thus before the multiple integrations of (10) and (11) can be executed, multiple integrations corresponding to every point Q' on the level surface are required to compute the input g^n. These practical integration concerns can be overcome by efficiently executing the whole scenario outlined in this section in the frequency domain. *Sideris* [1987] (also see *Sideris and Schwartz* [1986, 1988] for related works) uses analytically defined spectra, as well as discrete two-dimensional fast Fourier transforms (FFTs), to compute the convolutions of equations (9)–(11). This "analytical" approach will be summarized in the next section. An alternative approach, suggested by *Wang* [1988], is to compute all of the required spectra, including the geometrical kernels, via the discrete two-dimensional FFT pair. Experiments by this author have shown that use of the analytically defined transfer functions yield appreciably more accurate deflection predictions and thus will be incorporated in this paper.

Section 3 will discuss potential pitfalls in any use of the discrete two-dimensional FFT pair, highlighting the unwanted phenomena known as circular convolution. Finally, section 4 will examine sets of predicted deflections of the vertical in highly diverse topographic settings. Required input for the predictions are a truncated set of geopotential coefficients and gridded data bases of mean free-air gravity anomalies and elevations.

2. USING ANALYTICALLY DEFINED SPECTRA IN THE COMPUTATION OF EQUATIONS (9)–(11)

The spectrum of the rth vertical derivative of any two-dimensional planar gravimetric harmonic function $w(x, y, z = \text{const})$ is given by [cf. *Sideris*, 1987]

$$F\left\{\frac{\partial^r w(x, y, z = \text{const})}{\partial z^r}\right\} = (-2\pi q)^r W(f_x, f_y) \qquad (12)$$

where $W(f_x, f_y)$ denotes the Fourier transform of $w(x, y, z = \text{const})$ and

$$q = (f_x^2 + f_y^2)^{1/2} \tag{13}$$

with the linear frequencies f_x and f_y corresponding to the x and y directions. By treating each g^k as a planar harmonic function one has $L_1(g^k) = \partial g^k/\partial z$ and $L_r(g^k) = (1/r!)\partial^r(g^k)/\partial z^r$. Inserting (7) into (6) yields (in light of (12))

$$g_Q^n = -\sum_{r=1}^{n} z_Q^r \frac{1}{r!} F^{-1}\{(-2\pi q)^r G_Q^{n-r}\} \tag{14}$$

where G^k denotes the two-dimensional Fourier transform of g^k.

The well-known analytically defined spectra of the geometrical kernels of (11) are given by

$$F\left\{\frac{x}{[x^2 + y^2]^{3/2}}\right\} = \frac{-2\pi i f_x}{q} \tag{15}$$

and

$$F\left\{\frac{y}{[x^2 + y^2]^{3/2}}\right\} = \frac{-2\pi i f_y}{q} \tag{16}$$

for $q \neq 0$. For $q = 0$ both spectra are set equal to zero which corresponds to removing the mean of the kernel.

Linear convolution in the space domain corresponds to multiplication in the frequency domain provided the necessary steps are taken to convert periodic or circular convolutions, resulting from the use of the direct and inverse FFT, to the desired linear forms (see the next section for details). Hence the nth linear convolutions of (11) can be immediately expressed (in radians) as

$$\left\{\begin{array}{c} \xi_Q^n \\ \eta_Q^n \end{array}\right\} = -\frac{1}{\gamma} F^{-1}\left\{\begin{array}{c} (if_x/q)G_Q^n \\ (if_y/q)G_Q^n \end{array}\right\} \tag{17}$$

For a point A that resides on both the Earth's surface and the level surface (see Figure 1) the desired Earth surface deflections are simply given by

$$\left\{\begin{array}{c} \xi_A \\ \eta_A \end{array}\right\} = \sum_{n=0}^{\prime} \left\{\begin{array}{c} \xi_A^n \\ \eta_A^n \end{array}\right\} \tag{18}$$

with each ξ_A^n and η_A^n computed via (17). It is well-known that the analytical Fourier transform of $[x^2 + y^2]^{-1/2}$ is $1/q$ for $q \neq 0$, and it is again set to zero for $q = 0$. Hence the nth convolution of (10), evaluated (in meters) at an arbitrary Q' on the level surface, can be written as

$$\zeta_Q^n = \frac{1}{2\pi\gamma} F^{-1}\left\{\frac{1}{q} G_Q^n\right\} \tag{19}$$

and at A the desired Earth surface height anomaly is given by

$$\zeta_A = \sum_{n=0}^{\prime} \zeta_A^n \tag{20}$$

For arbitrary points P on the Earth's surface located below or above the level surface one can perform a Taylor series to

get back up (or back down) to P. One gets back to Δg_P from $\Delta g_{P'}$ via (1) which now can be written as

$$\Delta g_P = \sum_{n=0}^{\prime} g_P^n + \sum_{n=0}^{\prime} \left[z_P \frac{\partial g_{P'}^n}{\partial z} + \frac{z_P^2}{2!} \frac{\partial^2 g_{P'}^n}{\partial z^2} + \cdots \right] \tag{21}$$

Each $n \geq 1$ term in the first n-indexed summation is obtained from (14) (recall, by definition, $g_P^0 = \Delta g_P$). By treating each g^k as harmonic, it follows $\partial^r(g^k)/\partial z^r = F^{-1}\{G^k(-2\pi q)^r\}$, and through routine algebra one can easily show that the second n-indexed summation in (21), which has a starting index of zero, is equivalent to the following sum having a starting index of one:

$$\sum_{n=1}^{\prime} \bar{g}_P^n$$

where each

$$\bar{g}_P^n = +\sum_{r=1}^{n} \frac{1}{r!} z_P^r F^{-1}\{(-2\pi q)^r G_{P'}^{n-r}\} \tag{22}$$

Note that obviously, for $n \geq 1$, $\bar{g}_P^n = -g_P^n$ and (21) reduces to the defined $\Delta g_P = g_P^0$.

Similarly, if one treats each ζ^k, ξ^k, and η^k as planar harmonic functions, then it follows that

$$\partial^r(\zeta^k)/\partial z^r = [1/(2\pi\gamma)]F^{-1}\{(1/q)G^k(-2\pi q)^r\}$$
$$= (-1/\gamma)F^{-1}\{G^k(-2\pi q)^{r-1}\}$$
$$\partial^r(\xi^k)/\partial z^r = (1/\gamma)F^{-1}\{(-if_x/q)G^k(-2\pi q)^r\}$$
$$= (1/\gamma)F^{-1}\{G^k(-2\pi q)^{r-1}(2\pi i f_x)\}$$

and

$$\partial^r(\eta^k)/\partial z^r = (1/\gamma)F^{-1}\{(-if_y/q)G^k(-2\pi q)^r\}$$
$$= (1/\gamma)F^{-1}\{G^k(-2\pi q)^{r-1}(2\pi i f_y)\}$$

Taylor series akin to (21) can be expanded for ζ_P, ξ_P, and η_P. Equivalent to these expansions are the following final deflection expressions at any point P on the Earth's surface:

$$\left\{\begin{array}{c} \xi_P \\ \eta_P \end{array}\right\} = \sum_{n=0}^{\prime} \left\{\begin{array}{c} \xi_P^n \\ \eta_P^n \end{array}\right\} + \sum_{n=1}^{\prime} \left\{\begin{array}{c} \bar{\xi}_P^n \\ \bar{\eta}_P^n \end{array}\right\} \tag{23}$$

where

$$\left\{\begin{array}{c} \bar{\xi}_P^n \\ \bar{\eta}_P^n \end{array}\right\} = \frac{1}{\gamma} \sum_{r=1}^{n} \frac{1}{r!} z_P^r F^{-1}\left\{\begin{array}{c} (-2\pi q)^{r-1}(2\pi i f_x)G_{P'}^{n-r} \\ (-2\pi q)^{r-1}(2\pi i f_y)G_{P'}^{n-r} \end{array}\right\}$$

and the terms in the first n-indexed sum are obtained from (17). For the height anomaly one has

$$\zeta_P = \sum_{n=0}^{\prime} \zeta_P^n + \sum_{n=1}^{\prime} \bar{\zeta}_P^n \tag{24}$$

where
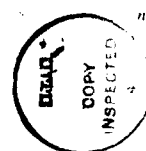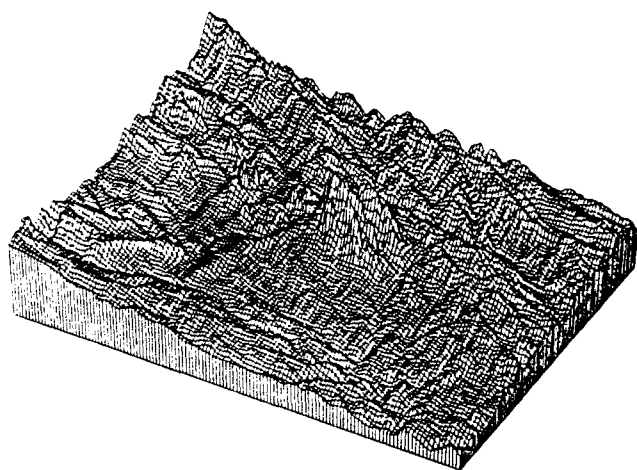
Fig. 2. The 1 arc min by 1 arc min topography (Oklahoma) of central 1.75° by 2.25° area.

$$\zeta_P^n = -\frac{1}{\gamma} \sum_{r=1}^{n} \frac{1}{r!} z_P^r F^{-1}\{(-2\pi q)^{r-1} G_{P'}^{n-r}\}$$

and the terms in the first n-indexed sum are obtained from (19). The fact that the efficient and simultaneous computation of the G^k spectra only has to be executed once (the G^k can be stored on a direct or random access disc file for future reference), together with the simultaneous calculation of gridded ζ, ξ, and η values via (23)–(24), constitute the appeal of Sideris' approach.

3. POTENTIAL PITFALLS OF THE DISCRETE FFT PAIR

Although some nice treatments of geodetic FFT techniques already exist [cf. Schwarz et al., 1990], the purpose of this section is to furnish a short (but detailed) explanation on the optimal computer execution of equations (23)–(24) using a direct or random access file of precomputed G^k spectra values obtained recursively from F {left-hand side of (14)}. First of all, most "canned" two-dimensional FFT routines such as International Mathematical and Statistical Library's (IMSL) FFT 3D expect the $\Delta g(0, 0)$ origin value to be at the southwest corner of the grid. Thus, to make inverse Fourier transforms such as (14), (23), and (24) amenable to such routines, one must apply the appropriate frequency shifts in any analytically-defined transfer function contributing to the final spectra which will be transformed back to the space domain by the inverse two-dimensional FFT routine.

There are three major areas of concern in any use of the discrete two-dimensional FFT pair, namely, aliasing, spectral leakage, and circular (nonlinear) convolution effects. Aliasing can only be truly eliminated by sampling the signal at a rate at least twice as high as the highest frequency present in the signal (if known). Thus one can only hope to minimize the aliasing effects by using as dense a grid of data as practically possible. A popular remedy [cf. Bergland 1969] for spectral leakage, resulting from the failure to examine the signal over its entire assumed period, is used here: namely, multiplying the given set of gridded free-air gravity anomalies by the well-known two-dimensional 80% cosine taper window. This eliminates discontinuities along the edges of the grid and allows the data to take on some

semblance of periodicity. Such a window must be applied to the actual data and not to any artificial data generated by filling out a record with zeros. Such artificial data will be discussed shortly and will be used in the test cases of section 4.

When the desired linear convolutions of (9)–(11) are computed with the aid of the discrete periodic FFT pair, such as in (14), (23), and (24), the resulting convolution is periodic or circular in two dimensions. To obtain the desired linear convolution, Oppenheim and Schafer [1975] show the dimensions of the two sequences to be convolved must be chosen large enough to avoid unwanted aliasing inherent to the periodic mode of the FFT pair. Convolution of two M by N sequences produces a sequence of area $2M$-1 by $2N$-1. Hence each array should be dimensioned $2M$ by $2N$ (or larger). Zero values are assigned to each location in the extended areas of the space domain g^k array. If one evaluates the spectra of the geometrical kernel or response function via a (southwest origin) two-dimensional discrete FFT, a "four corner" space domain grid assignment is made [see Oppenheim and Schafer, 1975] to avoid the "wrap-around" or circular convolution. Therein, the corner $N/2$ by $M/2$ nonzero sections of the overall $2N$ by $2M$ grid contain the appropriately shifted space domain kernel values and the rest of the grid is zero. One then takes the direct FFT of the extended $2M$ by $2N$ (or larger) grids. As alluded to earlier, somewhat better predictions occurred by using analytically-defined kernel spectra. Thus the analytically-defined transfer functions appearing in (14), (23), and (24) require "extended" frequency counter shifts (recall the transfer function frequencies must be shifted to adjust for the southwest origin). An inverse FFT of the extended product spectra is taken and the desired linear convolution is located in the original (nonextended) grid locations. Experiments have shown that neglecting the circular convolution effects can increase the error in individual deflection predictions by as much as 100% and increase the overall RMS of the prediction errors by several tenths of an arc second. An additional benefit of extending the original space domain g^k grid with zeros, to form a $2M$ by $2N$ grid, is the reduction of unwanted "picket fence" effects in the G^k spectra (see Bergland [1969] for more details). These unwanted effects, namely, the Fourier coefficients taking on the behavior of a set of overlapping band-pass filters, occur because the g^k signal does not consist of a desired set of purely discrete orthogonal frequencies.

4. TEST RESULTS

Sideris' two-step continuation scheme was subjected to all of the procedural steps outlined in section 3 to compute deflection of the vertical components from 1, 3, and 5 arc min gridded data bases of mean free-air gravity anomalies and mean terrain elevations in two areas having dramatically different topographies. The 1 arc min gridded files were furnished by the Defense Mapping Agency Aerospace Center (DMAAC), St. Louis, Missouri. The coarser 3 and 5 arc min files used were simply averaged versions of the 1 arc min data.

The north-south Δy planar sampling spacing, in meters, was set to an arc length of 1, 3, and 5 arc min along a meridian of radius 6371 km. The east-west Δx was set to Δy · $\cos \phi_M$, where ϕ_M is the middle-latitude value of the
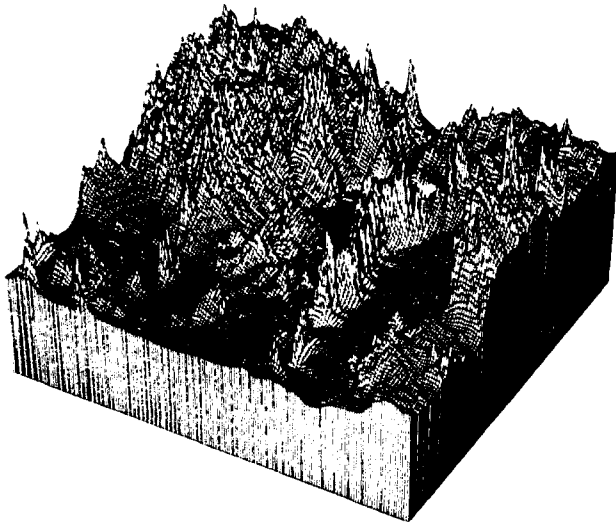
$$\cdot \sum_{m=0}^{n} (\bar{C}_{n,m}^{*} \cos m\lambda + \bar{S}_{n,m} \sin m\lambda) \bar{P}_{n,m}(\cos \theta) \qquad (25)$$

where θ denotes colatitude and the asterisk implies that the potential coefficients were made residual to the reference ellipsoid (various potential coefficient sets and values for NT were selected; the results will be discussed below). The geodetic $(\phi, \lambda, \text{height})_P$ coordinates are transformed to $(r, \theta, \lambda)_P$ geocentric coordinates before (25) is executed. The reduced set $\Delta g_{\text{reduced}} = \Delta g - \Delta g_{\text{removed}}$ was then subjected to the two step continuation scheme, producing a set of reduced deflection components. The long-wavelength features of the deflections were then added back via

$$\xi(r, \theta, \lambda) = \sum_{n=2}^{NT} \left(\frac{a}{r}\right)^{n+2}$$

$$\cdot \sum_{m=0}^{n} [\bar{C}_{n,m}^{*} \cos m\lambda + \bar{S}_{n,m} \sin m\lambda] \frac{d[\bar{P}_{n,m}(\cos \theta)]}{d\theta} \qquad (26)$$

and

$$\eta(r, \theta, \lambda) = \frac{-1}{\sin \theta} \sum_{n=2}^{NT} \left(\frac{a}{r}\right)^{n+2}$$

$$\cdot \sum_{m=0}^{n} m[-\bar{C}_{n,m}^{*} \sin m\lambda + \bar{S}_{n,m} \cos m\lambda] \bar{P}_{n,m}(\cos \theta) \qquad (27)$$

surveyed area. Predicted values were then compared to a set of astrogeodetic deflection "truth" values located in the center region of the surveyed area (noncentral predictions of course suffer from the shortened extent of the data and from the periodic nature of the FFT pair (with respect to the latter, see *Wang* [1988]).

The two areas selected were (1) the topographically tranquil but gravimetrically turbulent (due to the crustal density structure) Oklahoma/Texas test area of the Gravity Gradiometer Survey System and (2) the highly rugged White Sands, New Mexico, area. The input data bases for Oklahoma/Texas covered a 3.5° (north-south) by 4.5° (east-west) area and for New Mexico a 6° square area. Figure 2 illustrates the central 1.75° by 2.25° region of the Oklahoma site and Figure 3 illustrates the central 3° by 3° area of the New Mexico site (all astronomically determined "truth" stations were located in these central regions). Due to the rugged nature of the terrain, the accuracy of the New Mexico gravity anomalies is far from uniform. In inaccessible areas, a least squares collocation scheme was employed by DMAAC to obtain interpolated anomaly values.

The long-wavelength features of the Earth surface gravity anomalies corresponding to harmonic degrees $n \leq NT$ were removed by the spherical harmonic expansion

$$\Delta g_{\text{removed}}(r, \theta, \lambda) = \frac{\kappa M}{a^2} \sum_{n=2}^{NT} (n-1)\left(\frac{a}{r}\right)^{n+2}$$

For both areas the mean elevation surface was chosen as the level reference surface containing the points P' and Q' on Figure 1 (experiments revealed the n-indexed series of (5), (23), and (24) converge fastest for such a level surface choice). The final values ξ_k and η_k, to be compared to the kth astrogeodetic "truth" values, were obtained from a simple interpolation of the four predicted (gridded) deflections closest to the kth control point given by

$$\begin{Bmatrix} \xi_k \\ \eta_k \end{Bmatrix} = \frac{\displaystyle\sum_{i=1}^{4} \begin{Bmatrix} \xi_i/D_{ik} \\ \eta_i/D_{ik} \end{Bmatrix}}{\displaystyle\sum_{i=1}^{4} (1/D_{ik})} \qquad (28)$$

where D_{ik} is the planar distance from the control point k to the grid point i.

Fig. 3. The 1 arc min by 1 arc min topography (New Mexico) of central 3° by 3° area.

TABLE 1. Maximum g'', $\xi''(=\xi_P'' + \xi_P'')$, and $\eta''(=\eta_P'' + \eta_P'')$ Absolute Values, Given by (14) and (23), in Central Region of Surveyed Oklahoma/Texas Area

n	5 arc min by 5 arc min			3 arc min by 3 arc min			1 arc min by 1 arc min		
	g'', mGal	ξ'', arc sec	η'', arc sec	g'', mGal	ξ'', arc sec	η'', arc sec	g'', mGal	ξ'', arc sec	η'', arc sec
0	86.23	13.94	11.97	87.84	15.44	12.56	91.89	16.35	13.50
1	1.04	0.05	0.05	1.56	0.06	0.06	2.68	0.18	0.21
2	0.01	0.00	0.00	0.03	0.00	0.00	0.25	0.01	0.01
3	0.00	0.00	0.00	0.00	0.00	0.00	0.02	0.00	0.00

TABLE 2. Overall RMS Values of 24 (True – Predicted) ξ and η Differences for the Oklahoma/Texas Area

n Truncation Level of (23) n	5 arc min by 5 arc min ξ	5 arc min by 5 arc min η	3 arc min by 3 arc min ξ	3 arc min by 3 arc min η	1 arc min by 1 arc min ξ	1 arc min by 1 arc min η
0	0.56	0.42	0.44	0.42	0.35	0.32
1	0.55	0.41	0.43	0.42	0.34	0.32
2	0.55	0.41	0.43	0.42	0.34	0.32
3	0.55	0.41	0.43	0.42	0.34	0.32

The ξ and η differences are in arc seconds.

Note that the ξ_t "analytically continued" deflections represent the deviation of the actual plumb line from the normal plumb line at the ground point P, while the astrogeodetic ξ values denote its deviation from the perpendicular to the ellipsoidal footpoint of P. The difference is accounted for by the well-known normal reduction for the curvature of the plumb line [cf. *Heiskanen and Moritz*, 1967]. One has

$$\xi_{\text{astrogeodetic}} = \xi_{\text{analytically continued}} + f^* \frac{h}{R} \sin 2\phi \quad (29)$$

where f^* denotes the gravimetric flattening, R the radius of the spherical Earth, h the elevation of P, and ϕ its geodetic latitude.

For the Oklahoma/Texas area, use of the *Rapp* [1981] potential coefficient set through $NT = 36$ in equations (25)–(27) yielded the best quality predictions. Although such a truncation implies a 5° by 5° local data set is available (recall a 3.5° by 4.5° set was used), using higher degree coefficients was detrimental to the final predictions (*Sideris* [1987] cites similar experiences). Current high degree and order geopotential coefficient sets (such as Rapp's) are "combined" sets in the sense that the lower degree ($n \le 36$) coefficients are related to satellite observations, while the higher degree coefficients come from a global set of 1° or 30 arc min surface mean gravity anomalies. The latter coefficients are not as reliable as the former due to a scarcity of surface gravity information over large portions of the globe. Experiments revealed that use of dense, localized gravity anomaly data sets in conjunction with the satellite-related $n \le 36$ potential coefficients led to the best results.

Table 1 lists, for the 5, 3, and 1 arc min grids, the maximum g^n, ξ^n ($= \xi_p^n + \xi_p^n$) and η^n ($= \eta_p^n + \eta_p^n$), $n = 0$, 1, 2, 3, absolute values in the central region of the Oklahoma area. For such a tranquil topography, the higher-order terms are expectedly impotent (the significant g^1, ξ^1, and η^1 values (for the 1 arc min grid) were mainly located near the protruding hills appearing in the middle of Figure 2. The overall RMS (in arc seconds) of 24 (true – predicted) deflection differences in the Oklahoma/Texas area, for various grid resolutions and truncation levels of the n-indexed sums of equation (23), appear in Table 2. As expected, the higher-order terms contributed little to the final interpolated deflection computations. The average standard error of the astrogeodetic "truth" values was exceptionally low, ≈ 0.05 arc sec. The average standard errors of the input 1 arc min mean anomalies and elevations were 3.7 mGal and 30 m, respectively.

For the New Mexico site, the *Rapp* [1981] coefficient set was again used with $NT = 36$ to account for the long-wavelength contributions. Table 3 is the New Mexico counterpart to Table 1. The rugged New Mexico topography of Figure 3 is reflected in the large magnitudes of the Table 3 higher-order maximum absolute values. Extrapolating the 1 arc min by 1 arc min section of Table 3 (it was truncated at $n = 8$ due to a shortage of disk space at the Geophysics Laboratory (GL)) infers that equations (5) and (23) should be

TABLE 3. Maximum g^n, $\xi^n (=\xi_p^n + \xi_p^n)$, and $\eta^n (= \eta_p^n + \eta_p^n)$ Absolute Values, Given by (14) and (23), in Central Region of Surveyed New Mexico Area

n	5 arc min by 5 arc min g^n, mGal	5 arc min by 5 arc min ξ^n, arc sec	5 arc min by 5 arc min η^n, arc sec	3 arc min by 3 arc min g^n, mGal	3 arc min by 3 arc min ξ^n, arc sec	3 arc min by 3 arc min η^n, arc sec	1 arc min by 1 arc min g^n, mGal	1 arc min by 1 arc min ξ^n, arc sec	1 arc min by 1 arc min η^n, arc sec
0	119.80	11.88	28.76	137.52	12.94	28.47	155.81	15.72	33.03
1	19.56	0.75	1.07	31.61	1.15	1.69	85.79	2.19	3.51
2	3.31	0.06	0.16	8.74	0.15	0.38	72.47	0.79	1.16
3	0.41	0.01	0.02	1.89	0.03	0.08	60.44	0.49	0.88
4	0.04	0.00	0.00	0.33	0.01	0.01	44.63	0.28	0.80
5	0.00	0.00	0.00	0.05	0.00	0.00	28.54	0.16	0.60
6	0.00	0.00	0.00	0.01	0.00	0.00	15.83	0.11	0.41
7	0.00	0.00	0.00	0.00	0.00	0.00	7.69	0.07	0.26
8	0.00	0.00	0.00	0.00	0.00	0.00	3.31		

Fig. 4. The g^1 values of central $3° \times 3°$ New Mexico area, corresponding to 1 arc min × 1 arc min grid.
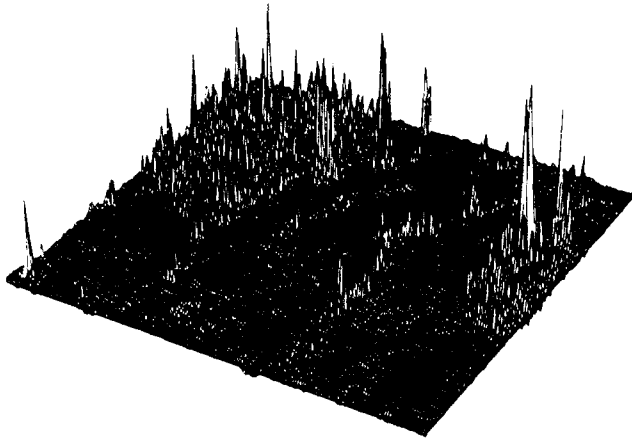

Fig. 6. The g^3 values of central $3° \times 3°$ New Mexico area, corresponding to 1 arc min × 1 arc min grid.

continued through $n = 10$ to obtain submilligal accuracies for the entire level surface $\Delta g'$ set and 0.1 arc sec accuracies for the Earth surface ξ and η sets. Such a truncation is far higher than reported by Sideris [1987] using 5 arc min by 5 arc min gridded data bases and interpolated 1 arc min grids. Wang [1988] also reports on the inability of interpolated grids to account for higher-frequency terrain effects. Figures 4, 5, and 6 plot the g^1, g^2, and g^3 values (vertical scale exaggerated) corresponding to the 1 arc min by 1 arc min grid, for the central $3°$ by $3°$ area of the New Mexico site.

Table 4 is the New Mexico counterpart to Table 2. As a preliminary remark, it should be mentioned that the 378 pairs of astrogeodetic deflections used are not part of an older astro set used by the well-known C. C. Tscherning White Sands Study Group and supplied by DMA's Geodetic Survey Squadron in Cheyenne, Wyoming. My initial experiments using the Tscherning astro values detected a bias of approximately 1.2 arc sec in the east-west η astro components. The Survey Squadron subsequently supplied me with a newer astro set having accuracies comparable to those of the Oklahoma set. The values appearing in Table 4 refer to this newer bias-free set. The tabular results agree closely with those obtained using the older astro set after the aforementioned east-west bias was removed.

Although the modest overall improvement in the predictions from the use of the 1 arc min by 1 arc min g^1 terms is
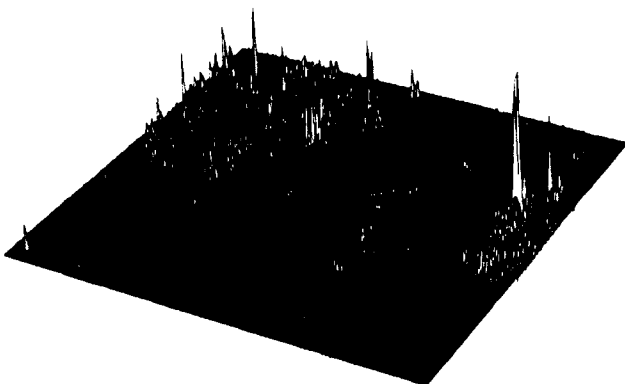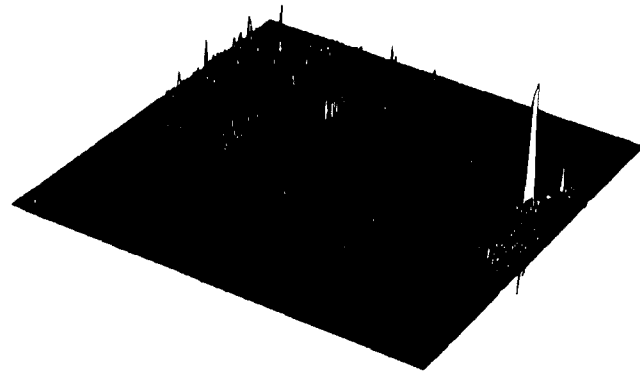

Fig. 5. The g^2 values of central $3° \times 3°$ New Mexico area, corresponding to 1 arc min × 1 arc min grid.

disappointing, it can readily be explained. Recall $g_P^1 = -z_P(\partial g^0/\partial z)_P$. As stated earlier, the majority of the total value of the anomalous vertical gradient is due to the behavior of g in the immediate 3 arc min area surrounding P. A 1 arc min grid supplies nine, 1 arc min by 1 arc min g^0 values in this area. For near-mountain astro stations having a dense sampling of actual point gravity measurements in this critical immediate 3 arc min area, the g^1 term consistently enhanced the predictions by several tenths of an arc second. By contrast, for near-mountain stations lacking such measurements, the g^1 term tended to deteriorate the predictions by comparable amounts. The overall statistic hides this significant g^1 activity and the use of interpolated anomalies in areas immediately surrounding the computation point is detrimental to the cause. Harrison and Dickinson [1989] suggest constructing a 30 arc sec grid (in this case) and placing the pertinent 1 arc min gravity and height values in each of the four 30 arc sec cells before computing the deflections. Execution of this suggestion with the given 1 arc min data sets did not improve the predictions.

In light of the above, one must question the accuracy of g^2 and higher terms obtained from a 1 arc min data grid. The g^2 term can justifiably be described as the "gradient of the gradient" of anomalous gravity. Clearly, the majority of its value is accounted for by the behavior of g in an immediate area far smaller than 3 arc min. Higher-order g^k terms are even more short wavelengthed. One must question how an initial set of 1 arc min mean anomalies and heights can account for all the high-frequency information in the to-be-solved-for g^k, even if the 1 arc min mean values are straight averages of a dense set of point measurements (i.e., they are interpolation-free). Moreover, noise (errors) present in the 1 arc min data will propagate into the computed, weak-signalled g^k and, in all probability, render them meaningless due to unacceptable signal/noise ratios. A 30 arc sec grid might allow for meaningful g^2 values provided interpolations are avoided (of course one runs into numerical stability, computer storage and CPU concerns with such a dense grid). By the same argument, if one is working with 3 or 5 arc min data grids, one is hard pressed to justify even the use of g^1. Notice in Table 4 that the overall RMS of the east-west η differences actually inched upward with the use of the 3 and 5 arc min g^1 values.

As a final remark, one can easily obtain a gridded set of deflections at a constant altitude h above the chosen level

TABLE 4. Overall RMS Values of 378 (True − Predicted) ξ and η Differences for the New Mexico Area

n Truncation Level of (23)	Grid Resolution					
	5 arc min by 5 arc min		3 arc min by 3 arc min		1 arc min by 1 arc min	
n	ξ	η	ξ	η	ξ	η
0	0.84	0.97	0.72	0.74	0.61	0.72
1	0.83	0.98	0.70	0.76	0.59	0.66
2	0.83	0.98	0.70	0.76	0.59	0.65
3	0.83	0.98	0.70	0.76	0.59	0.65

The ξ and η differences are in arc seconds.

surface through the routine spectral execution of the planar upward continuation integral given by

$$\{\xi(\text{at height } h)\} = F^{-1}\{X_A e^{-2\pi h q}\}$$

and

$$\{\eta(\text{at height } h)\} = F^{-1}\{H_A e^{-2\pi h q}\}$$

where X_A and H_A denote the two-dimensional Fourier transforms of the level surface ξ_A and η_A gridded sets given by (18) and $e^{-2\pi h q}$ is the well-known upward continuation transfer function.

5. SUMMARY

An efficient, spectrally implemented, density-free technique allows for the prediction of deflections of the vertical and height anomalies from input grids of free-air gravity anomalies and elevations. Long-wavelength contributions are accounted for by a low degree set of geopotential coefficients. The scheme has been successfully tested in two diverse topographies and accounts for severe terrain effects as well as turbulent gravimetric behavior due to crustal density structure. One minute grids of noninterpolated free-air gravity anomalies and heights are required for a universal set of accurate first-order vertical gradients of anomalous gravity, intermediate quantities in the prediction process. Accurate higher-order gradients will require even finer resolution grids of a noninterpolated nature.

REFERENCES

Bergland, G. D., A guided tour of the fast Fourier transform, *IEEE Spectrum*, 6, 41–52, 1969.

Bomford, G., *Geodesy*, Oxford at the Clarendon Press, London, 1971.

Harrison, J. C., and M. Dickinson, Fourier transform methods in local gravity modeling, *Bull. Geod.*, 63, 149–166, 1989.

Heiskanen, W. A., and H. Moritz, *Physical Geodesy*, W. H. Freeman, New York, 1967.

Moritz, H., *Advanced Physical Geodesy*, Abacus, Tunbridge Wells, Kent, Great Britain, 1980.

Oppenheim, A. V., and R. W. Schafer, *Digital Signal Processing*, Prentice-Hall, Englewood Cliffs, N. J., 1975.

Rapp, R. H., The Earth's gravity field to degree and order 180 using Seasat altimeter data, terrestrial gravity data and other data, *Rep. 322*, Dep. of Geod. Sci., Ohio State Univ., Columbus, 1981.

Schwarz, K. P., Data types and their spectral properties, in *Proceedings on Local Gravity Field Approximation*, Beijing International Summer School, Beijing, China, 1984.

Schwarz, K. P., M. Sideris, and R. Forsberg, The use of FFT techniques in physical geodesy, *Geophys. J.*, 100(3), 485–514, 1990.

Sideris, M. G., Spectral methods for the numerical solution of Molodensky's Problem, *Rep. 20024*, Dep. of Surv. Eng., Univ. of Calgary, Calgary, Alberta, Oct. 1987.

Sideris, M. G., and K. P. Schwarz, Solving Molodensky's problem by fast Fourier transform techniques, *Bull. Geod.*, 60, 51–63, 1986.

Sideris, M. G., and K. P. Schwarz, Advances in the numerical solution of the linear Molodensky problem, *Bull. Geod.*, 62, 59–69, 1988.

Wang, Y. M., Downward continuation of the free-air-gravity anomalies to the ellipsoidal using the gradient solution: Poisson's integral and terrain correction-numerical comparison and the computations, *Rep. 393*, Dep. of Geod. Sci. and Surv., Ohio State Univ., Columbus, June 1988.

D. M. Gleason, Geophysics Laboratory, Hanscom AFB, Bedford, MA 01731.

REPORT DOCUMENTATION PAGE			Form Approved OMB No. 0704-0188
1a. REPORT SECURITY CLASSIFICATION Unclassified		1b. RESTRICTIVE MARKINGS	
2a. SECURITY CLASSIFICATION AUTHORITY		3. DISTRIBUTION/AVAILABILITY OF REPORT Approved for public release; Distribution unlimited	
2b. DECLASSIFICATION/DOWNGRADING SCHEDULE			
4. PERFORMING ORGANIZATION REPORT NUMBER(S) GL-TR-90-0270		5. MONITORING ORGANIZATION REPORT NUMBER(S)	
6a. NAME OF PERFORMING ORGANIZATION Geophysics Laboratory	6b. OFFICE SYMBOL (If applicable) LWG	7a. NAME OF MONITORING ORGANIZATION	
6c. ADDRESS (City, State, and ZIP Code) Hanscom AFB Massachusetts 01731-5000		7b. ADDRESS (City, State, and ZIP Code)	
8a. NAME OF FUNDING/SPONSORING ORGANIZATION	8b. OFFICE SYMBOL (If applicable)	9. PROCUREMENT INSTRUMENT IDENTIFICATION NUMBER	
8c. ADDRESS (City, State, and ZIP Code)		10. SOURCE OF FUNDING NUMBERS	

PROGRAM ELEMENT NO. 61102F	PROJECT NO. 2309	TASK NO G1	WORK UNIT ACCESSION NO. 11

11. TITLE (Include Security Classification)
Obtaining Earth Surface and Spatial Deflections of the Vertical From Free-Air Gravity Anomaly and Elevation Data Without Density Assumption

12. PERSONAL AUTHOR(S)
David M. Gleason

13a. TYPE OF REPORT Reprint	13b. TIME COVERED FROM _____ TO _____	14. DATE OF REPORT (Year, Month, Day) 1990 October 12	15. PAGE COUNT 8

16. SUPPLEMENTARY NOTATION
Reprinted from Journal of Geophysical Research, Vol. 95, No. B5, Pages 6779-6786
May 10, 1990

17.	COSATI CODES		18. SUBJECT TERMS (Continue on reverse if necessary and identify by block number)
FIELD	GROUP	SUB-GROUP	Gravity anomaly, Deflection of the vertical, Upward continuation

19. ABSTRACT (Continue on reverse if necessary and identify by block number)

Moritz (1980) presents a density-free scheme allowing for the analytical or regular continuation of a given set of free-air gravity anomalies, referenced to the ground, to any desired level surface if a corresponding set of elevations (e.g., above mean sea level) is available. An efficient spectral implementation of this scheme is discussed by Sideris (1987). A subsequent spectral execution of the planar Vening-Meinez equation on the continued anomalies yields deflections of the vertical on the chosen level surface. The deflections are brought back to the Earth's surface via a spectrally implemented Taylor series. Deflections at a constant altitude above the level surface are obtained through a routine spectral execution of the planar upward continuation integral. Two sites, having diverse topographies, were surveyed for 1 arc min by 1 arc min mean free-air anomaly and elevation values and for smaller sets of astronomically determined deflections to serve as control or "truth" values. In a topographically tranquil but gravimetrically turbulent Oklahoma site the overall RMS of the differences between true and predicted deflections was 0.3 arc secs and in a rugged New Mexico site it was 0.6 arc sec. Accurate first derivative terms (in both continuation steps) require a 1 arc min data set as interpolation-free as possible. A 1 arc min data grid is shown to be insufficient for meaningful computations of the higher order series terms. Potential pitfalls of the two-dimensional fast Fourier transform pair are discussed with an emphasis on unwanted circular convolution effects which, if unaccounted for, can increase the error in individual predicted deflections by as much as 100%.

20. DISTRIBUTION/AVAILABILITY OF ABSTRACT ☐ UNCLASSIFIED/UNLIMITED ☒ SAME AS RPT. ☐ DTIC USERS	21. ABSTRACT SECURITY CLASSIFICATION Unclassified	
22a. NAME OF RESPONSIBLE INDIVIDUAL David M. Gleason	22b. TELEPHONE (Include Area Code) (617) 377-5255	22c. OFFICE SYMBOL LWG

DD Form 1473, JUN 86   Previous editions are obsolete.